NeuroImage 60 (2012) 1686–1695

Contents lists available at SciVerse ScienceDirect

NeuroImage

journal homepage: www.elsevier.com/locate/ynimg

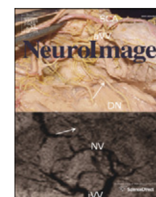

Full Length Article

# Genetic and environmental influences of white and gray matter signal contrast: A new phenotype for imaging genetics?

Matthew S. Panizzon [a,*], Christine Fennema-Notestine [a,b], Thomas S. Kubarych [c], Chi-Hua Chen [a], Lisa T. Eyler [a,d], Bruce Fischl [e,f,g], Carol E. Franz [a], Michael D. Grant [h], Samar Hamza [a], Amy Jak [a,d], Terry L. Jernigan [a,b,i], Michael J. Lyons [h], Michael C. Neale [c], Elizabeth C. Prom-Wormley [c], Larry Seidman [f], Ming T. Tsuang [a,j,k,l], Hao Wu [c], Hong Xian [m], Anders M. Dale [b,n], William S. Kremen [a,j,o]

[a] Department of Psychiatry, University of California, San Diego, La Jolla, CA 92093, USA
[b] Department of Radiology, University of California, San Diego, La Jolla, CA 92093, USA
[c] Virginia Institute for Psychiatric and Behavioral Genetics, Virginia Commonwealth University School of Medicine, Richmond, VA 23298, USA
[d] San Diego VA Health Care System, San Diego, CA 92161, USA
[e] Department of Radiology, Massachusetts General Hospital, Boston, MA 02114, USA
[f] Harvard Medical School, Boston, MA 02115, USA
[g] Computer Science and AI Lab, Massachusetts Institute of Technology, Cambridge, MA 02139, USA
[h] Department of Psychology, Boston University, Boston, MA 02215, USA
[i] Department of Cognitive Sciences, University of California, San Diego, La Jolla, CA 92093, USA
[j] Center for Behavioral Genomics, University of California, San Diego, La Jolla, CA 92093, USA
[k] Institute of Genomic Medicine, University of California, San Diego, La Jolla, CA 92093, USA
[l] Harvard Institute of Psychiatric Epidemiology and Genetics, Harvard Medical School and School of Public Health, Boston, MA 02115, USA
[m] Department of Medicine, Washington University School of Medicine, St. Louis, MO 63110, USA
[n] Department of Neurosciences, University of California, San Diego, La Jolla, CA 92093, USA
[o] VA Center of Excellence for Stress and Mental Health, San Diego, CA 92161, USA

ARTICLE INFO

*Article history:*
Received 25 April 2011
Revised 23 December 2011
Accepted 29 January 2012
Available online 8 February 2012

ABSTRACT

The estimation of cortical thickness is in part dependent on the degree of contrast in T1 signal intensity between white matter and gray matter along the cortical mantle. The ratio of white matter to gray matter signal (WM/GM contrast) has been found to vary as a function of age and Alzheimer's disease status, suggesting a biological component to what might otherwise be labeled as a nuisance variable. The aim of the present study was to determine if measures of WM/GM contrast are genetically influenced, as well as the degree to which this phenotype may be related to the genetic and environment determinants of cortical thickness. Participants were 514 male twins (130 monozygotic, 97 dizygotic pairs, and 60 unpaired individuals) from the Vietnam Era Twin Study of Aging. Ages ranged from 51 to 59 years. Measures of WM/GM contrast and cortical thickness were derived for 66 cortical regions of interest (ROI) using FreeSurfer-based methods. Univariate and bivariate twin analyses were used in order to estimate the heritability of WM/GM contrast, as well as the degree of shared genetic and environmental variance between WM/GM contrast and cortical thickness. WM/GM contrast was found to be significantly heritable in the majority of ROIs. The average heritability across individual ROIs was highest in the occipital lobe (.50), and lowest in the cingulate cortex (.24). Significant phenotypic correlations between WM/GM contrast and cortical thickness were observed for most of the ROIs. The majority of the phenotypic correlations were negative, ranging from −.11 to −.54. Of the 66 associations, only 17 significant genetic correlations were found, ranging from −.16 to −.34, indicating small amounts of shared genetic variance. The majority of the phenotypic correlations were accounted for by small unique environmental effects common between WM/GM contrast and cortical thickness. These findings demonstrate that like cortical thickness, WM/GM contrast is a genetically influenced brain structure phenotype. The lack of significant genetic correlations with cortical thickness suggests that this measure potentially represents a unique source of genetic variance, one that has yet to be explored by the field of imaging genetics.
© 2012 Elsevier Inc. All rights reserved.

## Introduction

The estimation of cortical thickness by manual or automated methods is dependent, to a large extent, on the degree of contrast

* Corresponding author at: Department of Psychiatry, University of California, San Diego, 9500 Gilman Drive (MC 0738), La Jolla, CA 9293-0738, USA. Fax: +1 858 822 5856.
*E-mail address:* mspanizz@ucsd.edu (M.S. Panizzon).

1053-8119/$ – see front matter © 2012 Elsevier Inc. All rights reserved.
doi:10.1016/j.neuroimage.2012.01.122

in signal intensity between white matter and gray matter along the cortical mantle (Fischl and Dale, 2000; Narr et al., 2005). Simply put, the greater the difference in signal intensities between these tissue types, resulting in a steeper signal gradient, the more precisely the gray–white boundary can be defined. This in turn leads to a more accurate determination of cortical thickness, particularly when done in three-dimensional space. Indeed, statistical adjustment for white matter to gray matter (WM/GM) signal contrast was recently shown to increase the effect size of cortical thickness differences related to Alzheimer's disease (AD) and improve the power to detect differences in cortical thickness due to normal aging (Westlye et al., 2009). While variability in magnetic field strength, pulse sequence, and data processing parameters can affect signal intensities in the white and gray matter, and thus influence the degree of WM/GM contrast (Han et al., 2006), there is growing evidence to suggest that this measure may also reflect intrinsic properties of the corresponding tissue.

Numerous studies have found that the ratio of white matter to gray matter signal varies as a function of increasing age, such that the degree of contrast declines later in life (Davatzikos and Resnick, 2002; Magnaldi et al., 1993; Raz et al., 1990; Salat et al., 2009; Westlye et al., 2009). Intriguingly, these contrast differences do not appear to be uniform throughout the cortex, but are predominant in the frontal, temporal, and parietal regions — areas that also demonstrate significant age-related changes in cortical thickness (Salat et al., 2009; Westlye et al., 2009). Regionally specific differences in WM/GM contrast have also been found when comparing AD to normal aging samples, suggesting that the measure may also be sensitive to AD-related neuropathology (Salat et al., 2011). The observed differences in signal contrast appear to be driven primarily by a gradual reduction in the white matter signal intensity, leading to speculation that the degree of WM/GM contrast is indicative of the integrity of the myelinated fibers that are present along the gray–white boundary (Salat et al., 2009, 2011; Westlye et al., 2009, 2010). The presence of such age- and disease-related effects strongly suggests that there is a biological component to what might otherwise be thought of as a technical nuisance variable resulting from hardware and acquisition parameters. This conclusion is speculative, however, as it remains unclear what precise mechanism is behind the observed changes in WM/GM contrast, or whether these effects stem from the same processes responsible for age-related changes in cortical thickness.

In the present study, we examined region-of-interest (ROI) based measures of WM/GM contrast in a sample of middle-aged male twins. Utilizing the classical twin design we first determined whether WM/GM contrast was itself a heritable phenotype; that is, are individual differences in the contrast measure partially attributable to genetic factors. Reviews of early twin and family MRI studies clearly demonstrate that structural aspects of the brain (e.g., whole brain volume, gray matter volume) are under substantial genetic influence (Peper et al., 2007; Schmitt et al., 2007a). More recent studies have expanded the range of structural phenotypes to include ROI and vertex-based measures of cortical thickness (Kremen et al., 2010; Lenroot et al., 2007; Rimol et al., 2009), cortical surface area (Eyler et al., 2011b; Panizzon et al., 2009; Winkler et al., 2010), as well as microstructural features of the brain's white matter obtained through diffusion tensor imaging (DTI) (Brouwer et al., 2010; Chiang et al., 2009, 2011; Kochunov et al., 2010). These studies have all found that structural brain phenotypes are under significant genetic influence. If the degree of WM/GM contrast along the cortical mantle is indicative of underlying genetic influences on tissue properties, then this measure, like the other brain phenotypes studied to date, should to some extent be heritable.

While the determination of whether or not a phenotype is heritable represents a critical step in establishing both its biological relevance and potential usefulness for future gene association studies, it is equally important to establish whether the observed genetic influences differ from those of other related phenotypes. Therefore, we also examined the degree to which measures of WM/GM contrast and cortical thickness possess common genetic and environmental influences. To date, relatively few genetically informative neuroimaging studies have examined the genetic and environmental relationships between brain phenotypes; however, those that have done so have found evidence for multiple distinct sources of genetic influence (Eyler et al., 2011a; Panizzon et al., 2009; Rimol et al., 2009; Schmitt et al., 2007b, 2008; Winkler et al., 2010). If WM/GM contrast and cortical thickness represent similar neuroanatomical features of the brain then a substantial degree of genetic overlap (i.e., shared genetic variance) should be present between them. Alternatively, the absence of genetic overlap would suggest that the phenotypes are biologically distinct from one another.

## Methods

### *Participants*

Data were obtained from participants in the first wave of the Vietnam Era Twin Study of Aging (VETSA), a longitudinal study of cognitive and brain aging with baseline in midlife (Kremen et al., 2006). Participants in the VETSA were drawn from the larger Vietnam Era Twin (VET) Registry, a nationally distributed sample of male-male twin pairs who served in the United States military at some point between 1965 and 1975 (Goldberg et al., 2002). Detailed descriptions of the VET Registry's method of ascertainment and demographic characteristics have been reported on previously (Eisen et al., 1987; Henderson et al., 1990). VETSA participants are all military veterans; however, the majority did not experience combat situations during their military careers. In total, 1237 men participated in the primary VETSA project. Participants were predominantly Caucasian (89.7%), with an average age of 55.4 years (SD = 2.5), and an average education of 13.8 years (SD = 2.1). In comparison to U.S. census data, participants in the VETSA are similar in health and demographic characteristics to American men in their age range (Centers for Disease Control and Prevention, 2003). As part of the primary VETSA project, participants traveled to either the University of California San Diego (UCSD) or Boston University for a daylong evaluation consisting of physical, psychosocial, and neurocognitive assessments. Beginning in year 3 of the VETSA, MRIs were conducted on either the day before or the day following these assessments at one of two scanning sites — the UCSD Medical Center or the Massachusetts General Hospital (MGH). Informed consent was obtained from all participants prior to their participation, and scanning protocols were approved by the institutional review boards at all participating universities and hospitals.

To be eligible for the primary VETSA project both members of a twin pair had to agree to participate and be between the ages of 51 and 59 at the time of recruitment. Approximately 6% of the individuals invited to participate in the MRI component of the VETSA declined. Additional participants were excluded from the MRI study for reasons such as metal in the body (7%), claustrophobia (3%), being unable to travel to the testing site (5%), the exclusion of their co-twin (9%), and equipment problems on the scanning day (8%). In the end, approximately 59% of the invited individuals participated in the MRI study. Analyses for the present study were based on data from 514 participants: 130 monozygotic (MZ) pairs, 97 dizygotic (DZ) pairs, and 60 unpaired individuals (i.e., participants whose co-twin could either not be scanned or whose data was not usable). Zygosity for 92% of the sample was determined by analysis of 25 satellite markers that were obtained from blood samples. For the remainder of the sample zygosity was determined through a combination of questionnaire and blood group methods (Eisen et al., 1989). Within the VETSA sample, a comparison of these two approaches has demonstrated a 95% agreement rate. Participants in the VETSA MRI study are similar to the larger VETSA sample with respect to age, education, ethnicity, employment status, and

self-reported health status (Kremen et al., 2010; Panizzon et al., 2009).

*Image acquisition*

We have previously described in detail the acquisition parameters and post-processing methods for the VETSA MRI study (Kremen et al., 2010). Briefly, images were acquired on Siemens 1.5 Tesla scanners. Scanning sequences were specifically designed to be compatible across different scanners and vendors. Sagittal T1-weighted MPRAGE sequences were utilized with a time to inversion of 1000 ms, a time echo of 3.31 ms, a time repetition of 2730 ms, a flip angle equal to 7°, a slice thickness of 1.33 mm, and a voxel size of 1.3 × 1.0 × 1.3 mm. Raw DICOM MRI files from both sites were downloaded to facilities at MGH for post-processing and quality control. Of the 530 scans available, quality control procedures excluded 16 due to either scanner artifact or technical errors in image processing.

*Image processing*

As detailed in our previous work (Kremen et al., 2010), cortical surface reconstruction was performed using methods based on the publicly available FreeSurfer software package (Dale et al., 1999; Fischl and Dale, 2000; Fischl et al., 1999, 2004a). Briefly, the explicit reconstruction of the cortical surface involves a number of subtasks, including correction of field inhomogeneities, creation of a normalized intensity image, and removal of non-brain tissue. The resulting surface is covered with a polygonal tessellation and smoothed to reduce metric distortions. The gray/white boundary is then locally defined as the point of the steepest change along the intensity gradient, thereby enabling cortical thickness to be estimated while allowing for variability in the degree of contrast between the white matter and gray matter. This surface is subsequently deformed outwards to obtain an explicit representation of the pial surface.

The surface was then divided into distinct cortical regions of interest, and each vertex was assigned a neuroanatomical label based on 1) the probability of each label at each location in a surface-based atlas space, 2) local curvature information, and 3) other contextual information (e.g., encoding spatial neighborhood relationships between labels) (Desikan et al., 2006; Fischl et al., 2004b). Similar to the methods described by Westlye and colleagues (Westlye et al., 2009), estimates of white matter and gray matter signal intensity were obtained at a distance of 0.2 mm from the gray–white boundary. The cortical surface was divided into 66 ROIs (33 per hemisphere) according the Desikan et al. (2006) parcellation scheme, and averages of the respective vertex values were derived for each region. Measures of WM/GM contrast were calculated by dividing each ROI's average white matter intensity value by the corresponding average gray matter intensity value.

*Statistical analysis*

In order to determine the relative influence of genetic and environmental factors on WM/GM contrast, we fit univariate biometrical models (also referred to as ACE models) to the data from each of the 66 ROIs. In the classical twin design the variance of a phenotype is decomposed into the proportion attributed to additive genetic (A) influences, common or shared environmental (C) influences (i.e., environmental factors that make members of a twin pair similar to one another), and unique environmental (E) influences (i.e., environmental factors that make members of a twin pair different from one another, including measurement error) (Eaves et al., 1978; Neale and Cardon, 1992). Additive genetic influences are assumed to correlate perfectly (1.0) between monogygotic (MZ) twins because they are genetically identical. Dizygotic (DZ) twins, on the other hand, share on average 50% of their segregating DNA, and are therefore assumed to correlate .50 for additive genetic influences. The shared environment is assumed to correlate 1.0 between both members of a twin pair, regardless of their zygosity. Unique environmental influences, by definition, are uncorrelated between the members of a twin pair. The proportion of the overall variance in a phenotype that is attributable to additive genetic influences is the heritability.

In addition we fit bivariate Cholesky decomposition models for each regional WM/GM contrast estimate and its corresponding cortical thickness estimate in order to determine if the two phenotypes share common genetic and environmental determinants. The "Cholesky" model decomposes the total covariance between phenotypes into genetic and environmental components; thus, the sum of the standardized genetic and environmental covariances is equal to the phenotypic correlation. The genetic and environmental covariance estimates can also be used to calculate genetic and environment correlations. In statistical terms, the genetic correlation between two phenotypes is equal to their genetic covariance, divided by the square root of the product of their separate genetic variances (Neale and Cardon, 1992). Shared environmental and unique environmental correlations are calculated in a similar fashion using the corresponding variance and covariance estimates. Conceptually, genetic correlations represent the degree to which genetic influences of one phenotype are predictive of the genetic influences for another phenotype (Carey, 1988); the analogous definition holds for environmental correlations. Because genetic and environmental correlations can have opposing signs, resulting in phenotypic correlations that are near zero, analyses were run for all ROIs regardless of the observed phenotypic correlation between WM/GM contrast and cortical thickness.

All analyses were performed using the raw data application of the maximum-likelihood based structural equation modeling software OpenMx (Boker et al., 2011). Measures of WM/GM contrast and cortical thickness were adjusted for the relative effects of age and scanner as part of the model fitting process. The inclusion of scanner in the model is critical to adjust for the influence of site-specific scanner hardware differences on measures of signal intensity and cortical thickness (Han et al., 2006). In the univariate analyses, the significance of the genetic and shared environment influences was tested by fixing the parameter in question to zero, and then comparing the resulting change in fit of the reduced model against that of the full model. No such test was performed for the unique environmental influences because this parameter must always be present in the model. Model comparisons were performed using the likelihood-ratio chi-square test (LRT), which was calculated as the difference in the −2 log likelihood (−2LL) of the reduced model from that of the full model. Non-significant LRT values ($p > .05$) indicate that a reduced model does not result in a significant change in fit relative to the comparison model, and thus provides a significance test for the parameter is question. Under certain regularity conditions, the LRT is distributed as a chi-square ($\chi^2$) with degrees of freedom (df) equal to the difference in the number of parameters between the two models (Steiger et al., 1985). However, because there is an implicit lower bound of zero for variance components, the distribution of the test statistics for the A and C parameters is distributed as a 50:50 mixture of zero and $\chi^2$ with df = 1 (Dominicus et al., 2006; Self and Liang, 1987). Failure to account for this mixed distribution produces p-values that are too large; however the issue is easily corrected by halving the p-values obtained from the naïve $\chi^2$ with df = 1 distribution. When the A and C parameters are tested simultaneously, the resulting distribution is a mixture of zero, $\chi^2$ with df = 1, and $\chi^2$ with df = 2 (Dominicus et al., 2006). In this case a more reasonable p-value can be obtained by halving the p-value generated from a $\chi^2$ with df = 1 distribution (Dominicus et al., 2006). Similar to the p-values, 95% confidence intervals are also affected by the boundary condition. We therefore utilized an adjustment developed by two of the co-authors (HW & MCN), which allowed the confidence intervals to be calculated in a fashion consistent with the

**Table 1**
Univariate ACE models for WM/GM contrast estimates and tests of nested models.

| Region of interest | $r_{mz}$ | $r_{dz}$ | Standardized variance components | | | | | | p-Values | | |
|---|---|---|---|---|---|---|---|---|---|---|---|
| | | | $a^2$ | 95% CI | $c^2$ | 95% CI | $e^2$ | 95% CI | No A | No C | No AC |
| *Frontal lobe* | | | | | | | | | | | |
| Superior frontal gyrus—L | .62 | .31 | .58 | (.24; .70) | .03 | (.00; .38) | .40 | (.30; .52) | .0020 | .4451 | <.0001 |
| Superior frontal gyrus—R | .61 | .28 | .59 | (.24; .69) | .00 | (.00; .36) | .41 | (.31; .53) | .0021 | .5000 | <.0001 |
| Middle frontal gyrus | | | | | | | | | | | |
| Rostral division—L | .48 | .14 | .45 | (.19; .57) | .00 | (.00; .38) | .55 | (.43; .69) | .0065 | .5000 | <.0001 |
| Rostral division—R | .51 | .20 | .48 | (.13; .59) | .00 | (.00; .38) | .52 | (.41; .66) | .0128 | .5000 | <.0001 |
| Caudal division—L | .59 | .23 | .58 | (.33; .68) | .00 | (.00; .36) | .42 | (.32; .54) | .0006 | .5000 | <.0001 |
| Caudal division—R | .61 | .18 | .59 | (.36; .69) | .00 | (.00; .35) | .41 | (.31; .53) | .0001 | .5000 | <.0001 |
| Inferior frontal gyrus | | | | | | | | | | | |
| Pars opercularis—L | .57 | .09 | .52 | (.32; .62) | .00 | (.00; .38) | .48 | (.38; .62) | .0005 | .5000 | <.0001 |
| Pars opercularis—R | .43 | .11 | .39 | (.11; .52) | .00 | (.00; .37) | .61 | (.48; .75) | .0177 | .5000 | <.0001 |
| Pars triangularis—L | .50 | .02 | .44 | (.26; .56) | .00 | (.00; .39) | .56 | (.44; .72) | .0011 | .5000 | <.0001 |
| Pars triangularis—R | .44 | .12 | .40 | (.08; .53) | .00 | (.00; .38) | .60 | (.47; .75) | .0240 | .5000 | <.0001 |
| Pars orbitalis—L | .33 | .20 | .18 | (.00; .45) | .13 | (.00; .39) | .69 | (.55; .84) | .2488 | .2938 | <.0001 |
| Pars orbitalis—R | .43 | .00 | .38 | (.19; .53) | .00 | (.00; .37) | .62 | (.47; .78) | .0043 | .5000 | <.0001 |
| Orbitofrontal cortex | | | | | | | | | | | |
| Lateral division—L | .56 | .17 | .49 | (.15; .61) | .00 | (.00; .39) | .51 | (.39; .63) | .0101 | .5000 | <.0001 |
| Lateral division—R | .58 | .05 | .52 | (.34; .64) | .00 | (.00; .36) | .48 | (.36; .61) | .0002 | .5000 | <.0001 |
| Medial division—L | .45 | .08 | .41 | (.16; .54) | .00 | (.00; .38) | .59 | (.46; .74) | .0097 | .5000 | <.0001 |
| Medial division—R | .55 | .20 | .51 | (.17; .62) | .00 | (.00; .40) | .49 | (.38; .62) | .0077 | .5000 | <.0001 |
| Frontal pole—L | .30 | −.08 | .24 | (.01; .38) | .00 | (.00; .30) | .76 | (.62; .89) | .0494 | .5000 | .0013 |
| Frontal pole—R | .26 | .09 | .24 | (.00; .39) | .00 | (.00; .30) | .76 | (.61; .90) | .1489 | .5000 | .0020 |
| Precentral gyrus—L | .70 | .21 | .66 | (.39; .74) | .00 | (.00; .34) | .34 | (.26; .45) | .0000 | .5000 | <.0001 |
| Precentral gyrus—R | .66 | .21 | .65 | (.42; .73) | .00 | (.00; .34) | .35 | (.27; .47) | .0000 | .5000 | <.0001 |
| Paracentral lobule—L | .43 | .10 | .41 | (.18; .54) | .00 | (.00; .39) | .59 | (.46; .75) | .0063 | .5000 | <.0001 |
| Paracentral lobule—R | .51 | .24 | .47 | (.09; .60) | .02 | (.00; .39) | .51 | (.40; .66) | .0214 | .4652 | <.0001 |
| *Cingulate cortex* | | | | | | | | | | | |
| Rostral anterior cingulate—L | .34 | .07 | .32 | (.04; .47) | .00 | (.00; .35) | .68 | (.53; .83) | .0378 | .5000 | .0001 |
| Rostral anterior cingulate—R | .38 | .09 | .33 | (.00; .46) | .00 | (.00; .35) | .67 | (.54; .82) | .1153 | .5000 | <.0001 |
| Caudal anterior cingulate—L | .28 | .08 | .26 | (.00; .40) | .00 | (.00; .31) | .74 | (.60; .88) | .0929 | .5000 | .0011 |
| Caudal anterior cingulate—R | .18 | .02 | .19 | (.00; .35) | .00 | (.00; .28) | .81 | (.65; .97) | .1216 | .5000 | .0234 |
| Rostral posterior division—L | .26 | .07 | .23 | (.00; .37) | .00 | (.00; .30) | .77 | (.63; .90) | .1955 | .5000 | .0018 |
| Rostral posterior division—R | .34 | .34 | .00 | (.00; .45) | .34 | (.04; .45) | .66 | (.54; .79) | .5000 | .0298 | <.0001 |
| Retrosplenial cortex—L | .33 | .08 | .29 | (.00; .42) | .00 | (.00; .33) | .71 | (.58; .85) | .1152 | .5000 | .0001 |
| Retrosplenial cortex—R | .35 | .14 | .28 | (.00; .45) | .03 | (.00; .38) | .68 | (.55; .84) | .1553 | .4530 | <.0001 |
| *Parietal lobe* | | | | | | | | | | | |
| Postcentral gyrus—L | .63 | .15 | .60 | (.37; .69) | .00 | (.00; .34) | .40 | (.31; .52) | .0001 | .5000 | <.0001 |
| Postcentral gyrus—R | .55 | .12 | .50 | (.26; .59) | .00 | (.00; .37) | .50 | (.41; .65) | .0020 | .5000 | <.0001 |
| Supramarginal gyrus—L | .53 | .15 | .48 | (.17; .60) | .00 | (.00; .38) | .52 | (.40; .65) | .0080 | .5000 | <.0001 |
| Supramarginal gyrus—R | .47 | .05 | .41 | (.19; .55) | .00 | (.00; .39) | .59 | (.45; .73) | .0055 | .5000 | <.0001 |
| Superior parietal cortex—L | .59 | .16 | .55 | (.32; .65) | .00 | (.00; .37) | .45 | (.35; .58) | .0007 | .5000 | <.0001 |
| Superior parietal cortex—R | .59 | .05 | .54 | (.35; .65) | .00 | (.00; .37) | .46 | (.35; .60) | .0001 | .5000 | <.0001 |
| Inferior parietal cortex—L | .48 | .02 | .42 | (.23; .55) | .00 | (.00; .39) | .58 | (.45; .73) | .0026 | .5000 | <.0001 |
| Inferior parietal cortex—R | .50 | .10 | .44 | (.18; .57) | .00 | (.00; .39) | .56 | (.43; .69) | .0075 | .5000 | <.0001 |
| Precuneus—L | .48 | .06 | .42 | (.19; .55) | .00 | (.00; .39) | .58 | (.45; .72) | .0062 | .5000 | <.0001 |
| Precuneus—R | .48 | .25 | .36 | (.00; .56) | .09 | (.00; .45) | .55 | (.44; .70) | .0681 | .3401 | <.0001 |
| *Occipital lobe* | | | | | | | | | | | |
| Lingual gyrus—L | .54 | .18 | .50 | (.21; .62) | .00 | (.00; .37) | .50 | (.38; .63) | .0049 | .5000 | <.0001 |
| Lingual gyrus—R | .59 | .29 | .46 | (.10; .65) | .09 | (.00; .46) | .45 | (.35; .58) | .0171 | .3406 | <.0001 |
| Pericalcarine cortex—L | .54 | −.03 | .46 | (.29; .59) | .00 | (.00; .36) | .54 | (.41; .67) | .0008 | .5000 | <.0001 |
| Pericalcarine cortex—R | .43 | .07 | .38 | (.12; .52) | .00 | (.00; .36) | .62 | (.48; .77) | .0153 | .5000 | <.0001 |
| Cuneus—L | .57 | .16 | .55 | (.33; .65) | .00 | (.00; .36) | .45 | (.35; .59) | .0004 | .5000 | <.0001 |
| Cuneus—R | .57 | .15 | .54 | (.29; .64) | .00 | (.00; .36) | .46 | (.36; .60) | .0011 | .5000 | <.0001 |
| Lateral occipital cortex—L | .62 | .18 | .58 | (.34; .67) | .00 | (.00; .36) | .42 | (.33; .55) | .0003 | .5000 | <.0001 |
| Lateral occipital cortex—R | .58 | .10 | .53 | (.32; .64) | .00 | (.00; .37) | .47 | (.36; .60) | .0007 | .5000 | <.0001 |
| *Temporal lobe* | | | | | | | | | | | |
| Lateral aspect | | | | | | | | | | | |
| Superior temporal gyrus—L | .44 | .05 | .39 | (.17; .52) | .00 | (.00; .38) | .61 | (.48; .77) | .0074 | .5000 | <.0001 |
| Superior temporal gyrus—R | .37 | .10 | .34 | (.03; .47) | .00 | (.00; .35) | .66 | (.53; .82) | .0406 | .5000 | <.0001 |
| Middle temporal gyrus—L | .48 | .09 | .45 | (.22; .56) | .00 | (.00; .37) | .55 | (.44; .71) | .0033 | .5000 | <.0001 |
| Middle temporal gyrus—R | .39 | .12 | .36 | (.01; .49) | .00 | (.00; .37) | .64 | (.51; .79) | .0437 | .5000 | <.0001 |
| Inferior temporal gyrus—L | .45 | .17 | .42 | (.07; .55) | .00 | (.00; .39) | .58 | (.45; .73) | .0269 | .5000 | <.0001 |
| Inferior temporal gyrus—R | .41 | .18 | .15 | (.00; .48) | .20 | (.00; .45) | .65 | (.52; .79) | .2940 | .2424 | <.0001 |
| Transverse temporal cortex—L | .31 | .08 | .29 | (.00; .45) | .00 | (.00; .33) | .71 | (.55; .85) | .0537 | .5000 | .0004 |
| Transverse temporal cortex—R | .37 | .17 | .36 | (.00; .47) | .00 | (.00; .36) | .64 | (.53; .81) | .0823 | .5000 | <.0001 |
| Banks sup. temporal sulcus—L | .33 | .21 | .24 | (.00; .46) | .08 | (.00; .38) | .68 | (.54; .84) | .1856 | .3604 | <.0001 |
| Banks sup. temporal sulcus—R | .24 | −.05 | .19 | (.00; .34) | .00 | (.00; .27) | .81 | (.66; .94) | .0926 | .5000 | .0086 |

*(continued on next page)*

**Table 1** (*continued*)

| Region of interest | $r_{mz}$ | $r_{dz}$ | Standardized variance components | | | | | | p-Values | | |
|---|---|---|---|---|---|---|---|---|---|---|---|
| | | | $a^2$ | 95% CI | $c^2$ | 95% CI | $e^2$ | 95% CI | No A | No C | No AC |
| Medial aspect | | | | | | | | | | | |
| Entorhinal cortex—L | .20 | .19 | .00 | (.00; .35) | .19 | (.00; .32) | .81 | (.66; .92) | .5000 | .1645 | .0034 |
| Entorhinal cortex—R | .25 | .02 | .22 | (.00; .39) | .00 | (.00; .30) | .78 | (.61; .91) | .0895 | .5000 | .0053 |
| Medial aspect | | | | | | | | | | | |
| Parahippocampal cortex—L | .40 | .22 | .35 | (.00; .53) | .04 | (.00; .40) | .61 | (.47; .77) | .0785 | .4264 | <.0001 |
| Parahippocampal cortex—R | .41 | .32 | .05 | (.00; .49) | .34 | (.00; .49) | .61 | (.49; .75) | .4240 | .0706 | <.0001 |
| Temporal pole—L | .39 | .07 | .35 | (.07; .48) | .00 | (.00; .36) | .65 | (.52; .81) | .0259 | .5000 | <.0001 |
| Temporal pole—R | .33 | .02 | .29 | (.04; .44) | .00 | (.00; .34) | .71 | (.56; .85) | .0350 | .5000 | .0003 |
| Fusiform gyrus—L | .49 | .18 | .46 | (.14; .57) | .00 | (.00; .38) | .54 | (.43; .69) | .0122 | .5000 | <.0001 |
| Fusiform gyrus—R | .47 | .17 | .44 | (.11; .55) | .00 | (.00; .39) | .56 | (.45; .71) | .0172 | .5000 | <.0001 |

$r_{mz}$ = correlation between monozygotic twins; $r_{dz}$ = correlation between dizygotic twins; $a^2$ = additive genetic influences; $c^2$ = shared/common environmental influences; $e^2$ = unique environmental influences; 95% CI = corrected 95% confidence intervals; no A = test of whether the additive genetic influences can be removed from the model; no C = test of whether the shared/common environmental influences can be removed from the model; no AC = test of whether both the additive genetic and shared/common environmental influences can be removed from the model.

adjusted p-values (Wu and Neale, submitted). Compared to an unadjusted CI, an adjusted CI has a higher lower limit if the point estimate is close to but not on its boundary of zero and has a higher upper limit if the point estimate of zero is obtained. The lower limit of the adjusted CI is always greater than zero when the adjusted test gives a significant result. Phenotypic, genetic and environmental correlations in the bivariate Cholesky models were also tested using the LRT method; however, due to the fact that these parameters do not involve a lower bound of zero, no adjustment of the p-values is required. Similarly, the 95% confidence intervals for these parameters required no correction.

## Results

WM/GM contrast values ranged from 1.081 in the right transverse temporal cortex to 1.147 in the left caudal anterior cingulate. On average, the cingulate cortex possessed the highest contrast estimates (1.127), while the occipital lobe possessed the lowest (1.096). Age had a minimal impact on the contrast values, with only 5 of the 66 ROIs demonstrating a significant effect ($p<.05$). Scanner, on the other hand, was found to have a significant impact on 60 of the 66 ROIs. Effect sizes (Cohen's *d*) for significant relationships ranged from .20 for the left lateral occipital cortex to .76 for the right caudal middle frontal gyrus. Average WM/GM contrast estimates, as well as the relative effects of age and scanner for all of the ROIs examined are presented in the supplemental materials (see Supplemental Table).

### *Heritability of white matter/gray matter signal contrast*

MZ and DZ cross-twin correlations, genetic and environmental variance components, as well as tests of significance for specific univariate model parameters are presented in Table 1. Heritability estimates ($a^2$) for the ROI-based measures of WM/GM contrast ranged from .00 for the right posterior cingulate and the left entorhinal cortex, to .66 for the left precentral gyrus. In total, 48 ROIs were significantly heritable in the full ACE model (i.e., additive genetic influences could be fixed at zero without a significant reduction in model fit). An additional 15 ROIs had heritability estimates that were substantially larger than zero, ranging from .17 to .36. These values reached statistical significance when the shared environmental influences were constrained to be zero, making it easier to detect significant genetic influences. Given that estimates of the shared environment were zero or near zero for the majority of ROIs, this constraint could be imposed without resulting in a significant change in model fit for all but one region. On average the heritability of individual ROIs was highest in the occipital lobe (average $a^2=.50$), followed by the parietal (average $a^2=.47$) and frontal lobes (average $a^2=.46$), the temporal lobes (average $a^2=.30$), and the cingulate cortex (average $a^2=.24$). Constraining both the genetic and shared environment parameter estimates to zero; in other words, testing a model in which only unique environmental influences accounted for the variance in WM/GM contrast, resulted in a significant change in model fit for all ROIs examined. Thus, the presence of significant familial influences on WM/GM contrast – influences attributable to either latent genetic factors or shared environmental factors – could be verified for every region.

In order to ensure no possible bias in the WM/GM contrast heritability estimates as the result of scanner differences, additional univariate analyses were performed excluding twin pairs discordant for scanning site. For these twin pairs, the different scanners would be expected to act as unique environmental factors, making the twins appear more dissimilar from one another. Should scanner effects still be present, their removal would be anticipated to increase heritability estimates by reducing unique environmental variance. Removing these subjects from the analyses resulted in an overall decrease in our heritability estimates. The resulting change in heritability was small; moreover, the changes were in the opposite direction of what would be expected. We therefore concluded that the presence of scanner-discordant twins in our data did not bias our heritability estimates. Results from these analyses are available from the corresponding author upon request.

### *Relationship between white matter/gray matter contrast and cortical thickness*

Phenotypic, genetic, and environmental correlations from the bivariate analysis of WM/GM contrast and cortical thickness, as well as tests of significance for each correlation are presented in Table 2. Given the small and non-significant effects of the shared environment on nearly all WM/GM contrast measures, as well as similar effects of the shared environment on previously reported upon estimates of cortical thickness (Kremen et al., 2010), the C parameters were constrained to be zero in all models. Significant phenotypic correlations were observed for 40 of the 66 ROIs examined. The majority of these correlations were negative, ranging from −.11 to −.54; however, some positive associations were also observed, ranging from .15 to .20. Overall, the average phenotypic correlation for all ROIs was −.09. In comparison, significant genetic correlations were observed for only 17 of the 66 ROIs examined. The genetic correlations ranged in magnitude from −.89 to .25, with only values in the negative range reaching statistical significance. The strongest significant genetic correlations were observed in the left and right pericalcarine cortices ($r_g=-.68$ and $-.89$, respectively), while the remaining significant correlations were dispersed across all of the major lobes. For the remaining bivariate models, the genetic correlation could be constrained to be zero without a significant reduction in fit ($p>.05$), indicating the presence of minimal shared genetic variance between WM/GM contrast and cortical thickness.

With respect to the unique environmental influences, 32 of the 66 ROIs were found to have significant unique environmental

**Table 2**
Phenotypic, genetic, and environmental correlations between WM/GM contrast and cortical thickness.

| Region of interest | Phenotypic correlations | | Genetic correlations | | Unique environment correlation | | p-Values | | |
|---|---|---|---|---|---|---|---|---|---|
| | $r_p$ | 95% CI | $r_g$ | 95% CI | $r_e$ | 95% CI | No $r_p$ | No $r_g$ | No $r_e$ |
| *Frontal lobe* | | | | | | | | | |
| Superior frontal gyrus—L | −.05 | (−.16; .06) | −.16 | (−.34; .01) | .18 | (.00; .34) | .0682 | .0668 | .0463 |
| Superior frontal gyrus—R | −.03 | (−.14; .08) | −.17 | (−.35; .01) | .22 | (.05; .38) | .0271 | .0689 | .0113 |
| Middle frontal gyrus | | | | | | | | | |
| Rostral division—L | .04 | (−.06; .15) | .10 | (−.18; .37) | .00 | (−.17; .17) | .7047 | .4839 | 1.000 |
| Rostral division—R | .02 | (−.08; .13) | −.09 | (−.34; .15) | .14 | (−.03; .30) | .2894 | .4424 | .1153 |
| Caudal division—L | .00 | (−.11; .11) | −.20 | (−.42; .01) | .27 | (.10; .42) | .0083 | .0644 | .0022 |
| Caudal division—R | −.01 | (−.11; .10) | −.17 | (−.38; .03) | .23 | (.06; .39) | .0253 | .0949 | .0080 |
| Inferior frontal gyrus | | | | | | | | | |
| Pars opercularis—L | .18 | (.07; .28) | .04 | (−.18; .25) | .36 | (.20; .50) | <.0001 | .6985 | <.0001 |
| Pars opercularis—R | .18 | (.08; .28) | .09 | (−.23; .38) | .23 | (.07; .38) | .0005 | .5485 | .0045 |
| Pars triangularis—L | .07 | (−.03; .18) | .13 | (−.16; .40) | .03 | (−.13; .20) | .3734 | .3652 | .6985 |
| Pars triangularis—R | .06 | (−.04; .16) | −.02 | (−.35; .28) | .12 | (−.05; .28) | .2645 | .8875 | .1573 |
| Pars orbitalis—L | −.22 | (−.31; −.12) | −.27 | (−.59; .09) | −.19 | (−.34; −.03) | .0001 | .1269 | .0221 |
| Pars orbitalis—R | −.11 | (−.21; −.01) | −.14 | (−.43; .17) | −.10 | (−.26; .08) | .0876 | .3681 | .2815 |
| Orbitofrontal cortex | | | | | | | | | |
| Lateral division—L | −.15 | (−.25; −.05) | −.24 | (−.48; .01) | −.07 | (−.24; .10) | .0177 | .0599 | .4274 |
| Lateral division—R | −.09 | (−.19; .02) | −.19 | (−.43; .06) | .01 | (−.17; .18) | .2276 | .1416 | .9203 |
| Medial division—L | −.28 | (−.37; −.19) | −.24 | (−.50; .10) | −.31 | (−.46; −.16) | <.0001 | .1463 | .0001 |
| Medial division—R | −.40 | (−.48; −.31) | −.64 | (−.86; −.42) | −.20 | (−.35; −.03) | <.0001 | <.0001 | .0210 |
| Frontal pole—L | −.19 | (−.28; −.09) | −.24 | (−.68; .24) | −.17 | (−.32; .00) | .0011 | .2857 | .0447 |
| Frontal pole—R | −.25 | (−.34; −.15) | .05 | (−1.0; 1.0) | −.31 | (−.45; −.16) | <.0001 | .8875 | .0001 |
| Precentral gyrus—L | −.15 | (−.25; −.04) | −.25 | (−.42; −.07) | .05 | (−.13; .22) | .0216 | .0069 | .5902 |
| Precentral gyrus—R | −.18 | (−.29; −.07) | −.33 | (−.50; −.15) | .10 | (−.08; .27) | .0016 | .0004 | .2857 |
| Paracentral lobule—L | −.16 | (−.26; −.06) | −.32 | (−.55; −.08) | .00 | (−.17; .17) | .0082 | .0081 | 1.000 |
| Paracentral lobule—R | −.23 | (−.33; −.13) | −.33 | (−.52; −.13) | −.11 | (−.28; .06) | .0001 | .0020 | .2031 |
| *Cingulate cortex* | | | | | | | | | |
| Rostral anterior cingulate—L | −.20 | (−.29; −.10) | −.37 | (−.81; .07) | −.13 | (−.28; .04) | .0006 | .0897 | .1237 |
| Rostral anterior cingulate—R | −.23 | (−.32; −.13) | −.13 | (−.48; .32) | −.27 | (−.40; −.11) | <.0001 | .5023 | .0007 |
| Caudal anterior cingulate—L | −.45 | (−.53; −.37) | −.57 | (−.87; −.15) | −.41 | (−.53; −.27) | <.0001 | .0186 | <.0001 |
| Caudal anterior cingulate—R | −.35 | (−.44; −.26) | −.62 | (−1.0; −.19) | −.26 | (−.41; −.10) | <.0001 | .0126 | .0021 |
| Rostral posterior division—L | −.01 | (−.11; .09) | .09 | (−.30; .52) | −.06 | (−.21; .11) | .7945 | .6315 | .5023 |
| Rostral posterior division—R | −.10 | (−.21; .00) | −.28 | (−.59; .02) | .01 | (−.16; .17) | .0963 | .0668 | .9203 |
| Retrosplenial cortex—L | −.05 | (−.15; .06) | .05 | (−.25; .37) | −.11 | (−.27; .05) | .3465 | .7401 | .1703 |
| Retrosplenial cortex—R | −.17 | (−.26; −.07) | −.30 | (−.60; .00) | −.09 | (−.24; .08) | .0054 | .0472 | .2965 |
| *Parietal lobe* | | | | | | | | | |
| Postcentral gyrus—L | −.06 | (−.17; .05) | −.20 | (−.40; .00) | .14 | (−.04; .30) | .1142 | .0528 | .1183 |
| Postcentral gyrus—R | −.22 | (−.32; −.11) | −.34 | (−.52; −.14) | −.06 | (−.23; .11) | .0003 | .0012 | .4976 |
| Supramarginal gyrus—L | .20 | (.10; .30) | .05 | (−.20; .26) | .36 | (.21; .50) | <.0001 | .6892 | <.0001 |
| Supramarginal gyrus—R | .15 | (.05; .25) | .03 | (−.25; .28) | .25 | (.09; .40) | .0011 | .8065 | .0027 |
| Superior parietal cortex—L | −.02 | (−.13; .09) | −.24 | (−.46; −.03) | .29 | (.12; .44) | .0028 | .0216 | .0010 |
| Superior parietal cortex—R | .06 | (−.05; .17) | −.07 | (−.28; .14) | .25 | (.07; .41) | .0171 | .5220 | .0059 |
| Inferior parietal cortex—L | .16 | (.05; .26) | .10 | (−.14; .33) | .23 | (.05; .39) | .0017 | .3897 | .0104 |
| Inferior parietal cortex—R | .20 | (.10; .30) | .17 | (−.09; .40) | .23 | (.07; .39) | .0001 | .1990 | .0061 |
| Precuneus—L | .15 | (.04; .25) | −.01 | (−.25; .22) | .33 | (.17; .47) | .0001 | 1.000 | .0001 |
| Precuneus—R | .18 | (.07; .28) | .09 | (−.15; .31) | .27 | (.11; .42) | .0002 | .4348 | .0014 |
| *Occipital lobe* | | | | | | | | | |
| Lingual gyrus—L | −.21 | (−.31; −.11) | −.20 | (−.41; .03) | −.23 | (−.39; −.06) | .0001 | .0853 | .0072 |
| Lingual gyrus—R | −.18 | (−.28; −.07) | −.34 | (−.55; −.14) | .04 | (−.13; .21) | .0027 | .0011 | .6171 |
| Pericalcarine cortex—L | −.52 | (−.59; −.44) | −.68 | (−.86; −.48) | −.39 | (−.53; −.24) | <.0001 | <.0001 | <.0001 |
| Pericalcarine cortex—R | −.54 | (−.61; −.47) | −.89 | (−1.0; −.68) | −.34 | (−.47; −.19) | <.0001 | <.0001 | <.0001 |
| Cuneus—L | −.10 | (−.21; .00) | −.06 | (−.28; .17) | −.16 | (−.32; .01) | .0550 | .6242 | .0706 |
| Cuneus—R | −.25 | (−.35; −.15) | −.18 | (−.37; .04) | −.34 | (−.48; −.18) | <.0001 | .1096 | .0001 |
| Lateral occipital cortex—L | −.21 | (−.31; −.11) | −.19 | (−.39; .02) | −.23 | (−.39; −.06) | .0001 | .0680 | .0071 |
| Lateral occipital cortex—R | −.16 | (−.27; −.06) | −.20 | (−.41; .03) | −.13 | (−.29; .04) | .0064 | .0864 | .1354 |
| *Temporal lobe* | | | | | | | | | |
| Lateral aspect | | | | | | | | | |
| Superior temporal gyrus—L | .04 | (−.07; .14) | −.07 | (−.34; .20) | .13 | (−.04; .30) | .2967 | .6101 | .1302 |
| Superior temporal gyrus—R | .10 | (−.01; .20) | .03 | (−.22; .27) | .17 | (.00; .33) | .0542 | .8065 | .0460 |
| Middle temporal gyrus—L | .17 | (.07; .27) | .25 | (−.04; .53) | .11 | (−.06; .27) | .0049 | .0848 | .1897 |
| Middle temporal gyrus—R | .10 | (−.01; .20) | −.07 | (−.39; .22) | .21 | (.04; .37) | .0253 | .6315 | .0140 |
| Inferior temporal gyrus—L | .06 | (−.04; .17) | .02 | (−.29; .29) | .10 | (−.07; .26) | .3499 | .8875 | .2636 |
| Inferior temporal gyrus—R | −.03 | (−.13; .08) | −.05 | (−.31; .21) | −.01 | (−.17; .15) | .8825 | .7184 | .9203 |
| Transverse temporal cortex—L | −.16 | (−.26; −.06) | −.22 | (−.51; .09) | −.14 | (−.30; .04) | .0055 | .1583 | .1245 |
| Transverse temporal cortex—R | −.11 | (−.22; −.01) | −.27 | (−.56; .01) | .00 | (−.17; .16) | .0696 | .0538 | 1.000 |
| Banks sup. temporal sulcus—L | −.06 | (−.16; .04) | .07 | (−1.0; 1.0) | −.08 | (−.24; .08) | .4296 | .8875 | .3009 |
| Banks sup. temporal sulcus—R | .09 | (−.01; .19) | .02 | (−.68; .67) | .11 | (−.05; .26) | .1800 | 1.000 | .1809 |

(continued on next page)

**Table 2** (*continued*)

| Region of interest | Phenotypic correlations | | Genetic correlations | | Unique environment correlation | | p-Values | | |
|---|---|---|---|---|---|---|---|---|---|
| | $r_p$ | 95% CI | $r_g$ | 95% CI | $r_e$ | 95% CI | No $r_p$ | No $r_g$ | No $r_e$ |
| Medial aspect | | | | | | | | | |
| Entorhinal cortex—L | −.31 | (−.40; −.22) | −.47 | (−.93; −.03) | −.26 | (−.40; −.10) | <.0001 | .0393 | .0016 |
| Entorhinal cortex—R | −.32 | (−.41; −.23) | −.58 | (−1.0; −.17) | −.22 | (−.37; −.06) | <.0001 | .0100 | .0066 |
| Parahippocampal cortex—L | −.16 | (−.26; −.05) | −.18 | (−.46; .12) | −.14 | (−.30; .03) | .0083 | .2146 | .1029 |
| Parahippocampal cortex—R | −.17 | (−.27; −.07) | −.29 | (−.52; −.05) | −.07 | (−.23; .10) | .0041 | .0198 | .4062 |
| Temporal pole—L | −.21 | (−.30; −.11) | −.33 | (−.62; −.04) | −.13 | (−.29; .04) | .0003 | .0275 | .1245 |
| Temporal pole—R | −.04 | (−.14; .06) | .20 | (−.25; .80) | −.12 | (−.28; .04) | .3296 | .3802 | .1371 |
| Fusiform gyrus—L | .08 | (−.02; .18) | .10 | (−.17; .36) | .07 | (−.10; .23) | .2982 | .4751 | .4424 |
| Fusiform gyrus—R | .05 | (−.06; .15) | −.13 | (−.39; .12) | .22 | (.05; .37) | .0408 | .3149 | .0122 |

$r_p$ = phenotypic correlation; $r_g$ = genetic correlation; $r_e$ = unique environment correlation; No $r_p$ = test of no phenotypic correlation between estimates of WM/GM contrast and cortical thickness; No $r_g$ = test of no genetic correlation; No $r_e$ = test of no unique environment correlation.

correlations between WM/GM contrast and cortical thickness, with roughly equal numbers of positive and negative relationships observed. The only areas that were found to demonstrate a consistent pattern of results were the left and right parietal lobes, where all but two ROIs were found to have significant unique environmental correlations. As was the case with the genetic correlations, the effects, although significant, were small and suggested only minimal shared unique environmental variance between the phenotypes.

## Discussion

In the present study we examined if the degree of signal contrast between white matter and gray matter along the cortical mantle could be utilized as a genetically-informative brain imaging phenotype, a role beyond its current relegation as a technical property of MRI. Our results demonstrate that WM/GM contrast is indeed genetically influenced, with significant heritability estimates ranging from .29 to .66. In addition, the genetic and environmental determinants of WM/GM contrast were found to be largely independent of those that influence cortical thickness (i.e., there was very little shared genetic variance between WM/GM contrast and cortical thickness). Although significant phenotypic correlations were observed for 40 out of the 66 ROIs examined, only 17 genetic correlations were found to be significant. In these cases the degree of shared genetic variance tended to be small and suggested more unique genetic influences rather than common genetic influences for the phenotypes. For the vast majority of regions examined, the genetic correlation between WM/GM contrast and cortical thickness could be constrained to be zero without a significant reduction in model fit. Thus, while the degree of WM/GM contrast is certainly critical to the accurate estimation of cortical thickness, it also has minimal genetic overlap with cortical thickness, suggesting that it captures additional genetic variance that is relevant to structural properties of the cerebral cortex.

The observed heritability estimates for WM/GM contrast were similar in magnitude to those for cortical thickness previously reported from the VETSA sample (Kremen et al., 2010). These heritability estimates ranged from .00 in the right rostral and left caudal divisions of the anterior cingulate, to .75 in the left superior frontal gyrus. Average heritability estimates for the ROIs within the major lobes were .53 for the occipital lobe, .49 for the frontal lobe, .60 for the parietal lobe, .40 for the temporal lobe, and .28 for the cingulate cortex. It is important to note that the heritability estimates for cortical thickness, as well as those for WM/GM contrast, possess relatively broad 95% confidence intervals. Thus, while it may be possible to state that for a few ROIs cortical thickness is statistically more genetically influenced than WM/GM contrast, or vice versa, this statement should not be generalized to the entire brain. Additional studies of the heritability of WM/GM contrast in other twin and family MRI samples are needed in order to more precisely determine the degree to which the phenotype is genetically influenced.

Recent cross-sectional studies spanning early to older adulthood have noted that age-related differences in WM/GM contrast, or equivalent measures, appear to be driven primarily by decreasing signal intensity within the white matter (Salat et al., 2009; Westlye et al., 2009), leading to speculation that WM/GM contrast is most influenced by the degree of myelination of white matter fibers under the cortical mantle. If this is truly the case, then it will be of interest to determine the degree of phenotypic, genetic, and environmental overlap between WM/GM contrast and indicators of white matter integrity derived from additional MRI sequences such as diffusion tensor imaging (DTI). Several studies have now demonstrated that phenotypes derived from DTI are heritable (Brouwer et al., 2010; Chiang et al., 2009, 2011; Kochunov et al., 2010); however, there has yet to be an examination of whether these measures are genetically or environmentally related to other brain imaging phenotypes. Should strong genetic overlap exist between WM/GM contrast measures and DTI-based measures, this could suggest that WM/GM contrast provides an indicator of white matter integrity for the fibers along the gray-white boundary. Alternatively, weak genetic overlap might suggest that WM/GM contrast captures unique structural properties that are not otherwise observable with other white matter imaging methods.

These results are derived from cross-sectional data; therefore, we cannot be certain as to whether the measures of WM/GM contrast obtained in the present study are reflective of age-related changes in the phenotype, or rather are indicative of longstanding (pre-existing) tissue properties. Measures of signal contrast have been shown to be highly sensitive to the effects of age in multiple samples, with the ratios of white matter to gray matter signal intensity (or vice versa) approaching 1.0 as participants get older (Davatzikos and Resnick, 2002; Magnaldi et al., 1993; Raz et al., 1990; Salat et al., 2009; Westlye et al., 2009). Moreover, the component elements of the measure, the white matter and gray matter signal intensities, both demonstrate inverted "U" shaped patterns when examined across the lifespan, suggesting that the phenotype undergoes substantial changes both during development and then again later in life (Westlye et al., 2010). That we observed little to no effect of age on WM/GM contrast in the present study was likely a product of our rather narrow age range of 51 to 59 years. Ongoing follow-up examination of this phenotype in the second wave of the VETSA project will be able to address whether the degree of WM/GM contrast changes over the course of late middle-age, as well as the role of genetic and environmental influences on those changes.

Despite using methods designed to be compatible across different scanners and vendors, we observed significant scanner effects for nearly all measures of WM/GM contrast. While such effects certainly influence the absolute measures of WM/GM contrast, their impact on the observed heritability estimates is likely negligible. The vast majority of participants in the VETSA (roughly 95%) were scanned at the same site as their co-twin; thus, any effect of scanner on WM/GM contrast would likely be observed as a shared/common environmental influence (i.e., something that makes twins more similar to

one another). By adjusting for scanner differences we eliminated any such effect and as a result made the heritability estimates (the statistic of primary interest in the present study) more precise. Statistical modeling of multi-site neuroimaging is an important area of work, and there have been a number of studies that have examined differences between scanners (including the effects of different vendors and different pulse sequences) that are important in this regard. While the more similar the initial sequence and scanner are, the more similar the resultant measures, recent work has shown that combining data from multiple sites is feasible and provides sufficient power to look at these questions, particularly when site or scanner is used as a covariate in the model (Fennema-Notestine et al., 2007; Jack et al., 2008; Kruggel et al., 2010; Stonnington et al., 2008)

There are several limitations to the present study that should be addressed. With the all-male, largely Caucasian composition of the VETSA sample, we are limited in our ability to generalize these findings to other populations. Similarly, the results observed for this sample may differ from those obtained in either younger or older cohorts where individual differences in WM/GM contrast could be markedly greater or reduced as a function of age. Although our generalizability to other groups may be limited, it should be noted that the goal of the VETSA was to characterize men in a narrow midlife age range and then follow them as they age. Thus, the ability to examine aging-related phenotypes within a specific age cohort should also be viewed as a strength of the study's design. It is also the case that these results are not necessarily generalizable to other studies that do not use inversion recovery sequences, and the results may reflect an underestimation of age-related effects on WM/GM contrast relative to studies utilizing classical spoiled gradient echo sequences. Nevertheless, the methods used in the current study are similar, if not identical to those used by other researchers who have recently utilized contrast phenotypes to demonstrate subtle brain changes associated with normal aging and AD (Salat et al., 2009, 2011; Westlye et al., 2009, 2010). There may also be some measurement error introduced in our boundary estimation due to our anisotropic sampling, particularly when reslicing into isotropic volumes. Previous work suggests that anisotropic acquisitions may result in a bias to underestimate cortical thickness across the surface (Wonderlick et al., 2009). Our use of sinc interpolation in resampling preserves most of the original image information without further image degradation or blurring, and therefore reduces the impact of this problem on our estimates of cortical thickness and WM/GM contrast. The methodological approach used herein is similar to many previous studies of independent samples that have demonstrated sensitivity to subtle effects, thus supporting the utility of the measures derived from images with comparable voxel size (e.g., Dickerson et al., 2008; Fennema-Notestine et al., 2009; Fjell et al., 2009; Salat et al., 2004).

Finally, it is possible that the voxel size utilized in the present study ($1.3 \times 1.0 \times 1.3$ mm) may influence the heritability of the WM/GM contrast phenotype, and that a smaller voxel size could result in a more refined heritability estimate[1]. Given that this is the first study to report on the heritability of WM/GM contrast, no direct comparisons are possible; however, insights may be gleaned from the comparison of the heritability estimates from the VETSA (Kremen et al., 2010) with those from a subsequent genetically-informative study. In the Genetics of Brain Structure and Function Study (GOBS), an independent sample of family-based neuroimaging data, the heritability of cortical thickness was examined utilizing the same parcellation system as the VETSA with a voxel size of 0.8 $mm^3$ (Winkler et al., 2010). Similar to the VETSA, the ROI-based heritability estimates for cortical thickness in the GOBS demonstrated a wide range (.12 to .84; .00 to .75 in VETSA), with a roughly comparable average of the heritability estimates for all ROIs (VETSA = .46; GOBS = .41). Average heritability estimates for cortical thickness at the lobar level were also comparable across samples (frontal: VETSA = .49, GOBS = .37; temporal: VETSA = .40, GOBS = .41; parietal: VETSA = .60, GOBS = .50; occipital: VETSA = .53, GOBS = .44; cingulate cortex: VETSA = .28, GOBS = .37). Three of these estimates were slightly higher in the VETSA and two were slightly higher in the Winkler et al. study. These values indicate no systematic differences in the heritability estimates of the two studies, despite the differences in voxel size. Thus, the evidence argues against voxel size leading to systematically different heritability estimates for WM/GM contrast.

In addition to the above limitations, it is worth noting that conclusions drawn about the regionality of genetic and environmental determinants of WM/GM contrast may be influenced by the type of cortical parcellation system utilized. In previous studies by our group we demonstrated that heritability estimates of cortical thickness and cortical surface area derived from continuous maps of the cortical surface did not correspond to a priori ROI definitions (Chen et al., 2011; Rimol et al., 2009). This approach does not invalidate the use of cortical parcellation systems, which have established functional and anatomical significance, but rather highlights the fact that patterns of genetic and environmental influences may not adhere to predefined boundaries despite the established functional and anatomical significance of many cortical parcellation systems. Imposing these boundaries on the data may, therefore, introduce additional error into the results, subsequently reducing the heritability estimates.

In summary, the present results demonstrate that WM/GM contrast is both a heritable phenotype, and is largely genetically independent from cortical thickness. We conclude that WM/GM contrast may represent a novel phenotype with which to investigate the genetic determinants of brain structure and brain aging. Further studies are needed in order to replicate the findings in other populations and to determine how the genetic influences of WM/GM contrast may change throughout the lifespan.

## Disclosure statement

Dr. Anders M. Dale is a founder and holds equity in CorTechs Laboratories, Inc., and also serves on the Scientific Advisory Board. The terms of this arrangement have been reviewed and approved by the University of California, San Diego in accordance with its conflict of interest policies. All other authors state that there are no actual or potential conflicts of interest.

## Acknowledgments

The VETSA project is supported by National Institutes of Health/National Institute on Aging (NIH/NIA) Grants R01 AG18386, RO1 AG18384, RO1 AG22381, and RO1 AG22982. The U.S. Department of Veterans Affairs has provided support for the development and maintenance of the Vietnam Era Twin Registry. Numerous organizations have provided invaluable assistance, including VA Cooperative Studies Program; VA Center of Excellence for Stress and Mental Health; Department of Defense; National Personnel Records Center, National Archives and Records Administration; the Internal Revenue Service; National Institutes of Health; National Opinion Research Center; National Research Council, National Academy of Sciences; the Institute for Survey Research, Temple University; Schulman, Ronca, and Bucuvalas, Inc. Most importantly, we gratefully acknowledge the cooperation and participation of the members of the Vietnam Era Twin Registry and their families. Without their contribution this research would not have been possible.

## Appendix A. Supplementary data

Supplementary data to this article can be found online at doi:10.1016/j.neuroimage.2012.01.122.

[1] This issue was raised by an anonymous reviewer.

## References

Boker, S., Neale, M.C., Maes, H.H., Wilde, M., Spiegel, M., Brick, T., Spies, J., Estabrook, R., Kenny, S., Bates, T., Mehta, P.H., Fox, J., 2011. OpenMx: an open source extended structural equation modeling framework. Psychometrika 76, 306–317.
Brouwer, R.M., Mandl, R.C., Peper, J.S., van Baal, G.C., Kahn, R.S., Boomsma, D.I., Hulshoff Pol, H.E., 2010. Heritability of DTI and MTR in nine-year-old children. NeuroImage 53, 1085–1092.
Carey, G., 1988. Inference about genetic correlations. Behav. Genet. 18, 329–338.
Centers for Disease Control and Prevention, 2003. Public health and aging: trends in aging—United States and worldwide. MMWR CDC Surveill. Summ. 52, 101–106.
Chen, C.H., Panizzon, M.S., Eyler, L.T., Jernigan, T.L., Thompson, W., Fennema-Notestine, C., Jak, A.J., Neale, M.C., Franz, C.E., Hamza, S., Lyons, M.J., Grant, M.D., Fischl, B., Seidman, L.J., Tsuang, M.T., Kremen, W.S., Dale, A.M., 2011. Genetic influences on cortical regionalization in the human brain. Neuron 72, 537–544.
Chiang, M.C., Barysheva, M., Shattuck, D.W., Lee, A.D., Madsen, S.K., Avedissian, C., Klunder, A.D., Toga, A.W., McMahon, K.L., de Zubicaray, G.I., Wright, M.J., Srivastava, A., Balov, N., Thompson, P.M., 2009. Genetics of brain fiber architecture and intellectual performance. J. Neurosci. 29, 2212–2224.
Chiang, M.C., McMahon, K.L., de Zubicaray, G.I., Martin, N.G., Hickie, I., Toga, A.W., Wright, M.J., Thompson, P.M., 2011. Genetics of white matter development: a DTI study of 705 twins and their siblings aged 12 to 29. NeuroImage 54, 2308–2317.
Dale, A.M., Fischl, B., Sereno, M.I., 1999. Cortical surface-based analysis. I: segmentation and surface reconstruction. NeuroImage 9, 179–194.
Davatzikos, C., Resnick, S.M., 2002. Degenerative age changes in white matter connectivity visualized in vivo using magnetic resonance imaging. Cereb. Cortex 12, 767–771.
Desikan, R.S., Segonne, F., Fischl, B., Quinn, B.T., Dickerson, B.C., Blacker, D., Buckner, R.L., Dale, A.M., Maguire, R.P., Hyman, B.T., Albert, M.S., Killiany, R.J., 2006. An automated labeling system for subdividing the human cerebral cortex on MRI scans into gyral based regions of interest. NeuroImage 31, 968–980.
Dickerson, B.C., Fenstermacher, E., Salat, D.H., Wolk, D.A., Maguire, R.P., Desikan, R., Pacheco, J., Quinn, B.T., Van der Kouwe, A., Greve, D.N., Blacker, D., Albert, M.S., Killiany, R.J., Fischl, B., 2008. Detection of cortical thickness correlates of cognitive performance: reliability across MRI scan sessions, scanners, and field strengths. NeuroImage 39, 10–18.
Dominicus, A., Skrondal, A., Grjessing, H.K., Pedersen, N.L., Palmgren, J., 2006. Likelihood ratio tests in behavioral genetics: problems and solutions. Behav. Genet. 36, 331–340.
Eaves, L.J., Last, K.A., Young, P.A., Martin, N.G., 1978. Model-fitting approaches to the analysis of human behavior. Heredity 41, 249–320.
Eisen, S.A., Neuman, R., Goldberg, J., Rice, J., True, W., 1989. Determining zygosity in the Vietnam Era Twin Registry: an approach using questionnaires. Clin. Genet. 35, 423–432.
Eisen, S.A., True, W.R., Goldberg, J., Henderson, W., Robinette, C.D., 1987. The Vietnam Era Twin (VET) Registry: method of construction. Acta Genet. Med. Gemellol. 36, 61–66.
Eyler, L.T., Prom-Wormley, E., Fennema-Notestine, C., Panizzon, M.S., Neale, M.C., Jernigan, T.L., Fischl, B., Franz, C.E., Lyons, M.J., Stevens, A., Pacheco, J., Perry, M.E., Schmitt, J.E., Spitzer, N.C., Seidman, L., Thermenos, H.W., Tsuang, M., Dale, A., Kremen, W.S., 2011a. Genetic patterns of correlation among subcortical volumes in humans: results from a magnetic resonance imaging tiwn study. Hum. Brain Mapp. 32, 641–653.
Eyler, L.T., Prom-Wormley, E., Panizzon, M.S., Kaup, A.R., Fennema-Notestine, C., Neale, M.C., Jernigan, T.L., Fischl, B., Franz, C.E., Lyons, M.J., Grant, M., Stevens, A., Pacheco, J., Perry, M.E., Schmitt, J.E., Seidman, L.J., Thermenos, H.W., Tsuang, M.T., Chen, C.H., Thompson, W.K., Jak, A., Dale, A.M., Kremen, W.S., 2011b. Genetic and environmental contributions to regional cortical surface area in humans: a magnetic resonance imaging twin study. Cereb. Cortex 21, 2313–2321.
Fennema-Notestine, C., Gamst, A.C., Quinn, B.T., Pacheco, J., Jernigan, T.L., Thal, L., Buckner, R., Killiany, R., Blacker, D., Dale, A.M., Fischl, B., Dickerson, B., Gollub, R.L., 2007. Feasibility of multi-site clinical structural neuroimaging studies of aging using legacy data. Neuroinformatics 5, 235–245.
Fennema-Notestine, C., Hagler, D.J., McEvoy, L.K., Fleisher, A.S., Wu, E.H., Karow, D.S., Dale, A.M., 2009. Structural MRI biomarkers for preclinical and mild Alzheimer's disease. Hum. Brain Mapp. 30, 3238–3253.
Fischl, B., Dale, A.M., 2000. Measuring the thickness of the human cerebral cortex from magnetic resonance images. Proc. Natl. Acad. Sci. U. S. A. 97, 11050–11055.
Fischl, B., Salat, D.H., van der Kouwe, A.J., Makris, N., Segonne, F., Quinn, B.T., Dale, A.M., 2004a. Sequence-independent segmentation of magnetic resonance images. NeuroImage 23, S69–S84.
Fischl, B., Sereno, M.I., Dale, A.M., 1999. Cortical surface-based analysis. II: inflation, flattening, and a surface-based coordinate system. NeuroImage 9, 195–207.
Fischl, B., van der Kouwe, A., Destrieux, C., Halgren, E., Segonne, F., Salat, D.H., Busa, E., Seidman, L.J., Goldstein, J., Kennedy, D., Caviness, V., Makris, N., Rosen, B., Dale, A.M., 2004b. Automatically parcellating the human cerebral cortex. Cereb. Cortex 14, 11–22.
Fjell, A.M., Walhovd, K.B., Fennema-Notestine, C., McEvoy, L.K., Hagler, D.J., Holland, D., Brewer, J.B., Dale, A.M., 2009. One-year brain atrophy evident in healthy aging. J. Neurosci. 29, 15223–15231.
Goldberg, J., Curran, B., Vitek, M.E., Henderson, W.G., Boyko, E.J., 2002. The Vietnam Era Twin Registry. Twin Res. Hum. Genet. 5, 476–481.
Han, X., Jovicich, J., Salat, D., van der Kouwe, A., Quinn, B., Czanner, S., Busa, E., Pacheco, J., Albert, M., Killiany, R., Maguire, P., Rosas, D., Makris, N., Dale, A., Dickerson, B., Fischl, B., 2006. Reliability of MRI-derived measurements of human cerebral cortical thickness: the effects of field strength, scanner upgrade and manufacturer. NeuroImage 32, 180–194.
Henderson, W.G., Eisen, S.E., Goldberg, J., True, W.R., Barnes, J.E., Vitek, M., 1990. The Vietnam Era Twin Registry: a resource for medical research. Public Health Rep. 105, 368–373.
Jack, C.R., Bernstein, M.A., Fox, N.C., Thompson, P., Alexander, G., Harvey, D., Borowski, B., Britson, P.J., Whitwell, J.L., Ward, C., Dale, A.M., Felmlee, J.P., Gunter, J.L., Hill, D.L., Killiany, R., Schuff, N., Fox-Bosetti, S., Lin, C., Studholme, C., DeCarli, C.S., Krueger, G., Ward, H.A., Metzger, G.J., Scott, K.T., Mallozzi, R., Blezek, D., Levy, J., Debbins, J.P., Fleisher, A.S., Albert, M., Green, R., Bartzokis, G., Glover, G., Mugler, J., Weiner, M.W., 2008. The Alzheimer's Disease Neuroimaging Initiative (ADNI): MRI methods. J. Magn. Reson. Imaging 27, 685–691.
Kochunov, P., Glahn, D.C., Lancaster, J.L., Winkler, A.M., Smith, S., Thompson, P.M., Almasy, L., Duggirala, R., Fox, P.T., Blangero, J., 2010. Genetics of microstructure of cerebral white matter using diffusion tensor imaging. NeuroImage 53, 1109–1116.
Kremen, W.S., Prom-Wormley, E., Panizzon, M.S., Eyler, L.T., Fischl, B., Neale, M.C., Franz, C.E., Lyons, M.J., Pacheco, J., Perry, M.E., Stevens, A., Schmitt, J.E., Grant, M.D., Seidman, L.J., Thermenos, H.W., Tsuang, M.T., Eisen, S.A., Dale, A.M., Fennema-Notestine, C., 2010. Genetic and environmental influences on the size of specific brain regions in midlife: the VETSA MRI study. NeuroImage 49, 1213–1223.
Kremen, W.S., Thompson-Brenner, H., Leung, Y.J., Grant, M.D., Franz, C.E., Eisen, S.A., Jacobson, K.C., Boake, C., Lyons, M.J., 2006. Genes, environment, and time: The Vietnam Era Twin Study of Aging (VETSA). Twin Res. Hum. Genet. 9, 1009–1022.
Kruggel, F., Turner, J., Muftuler, L.T., 2010. Impact of scanner hardware and imaging protocol on image quality and compartment volume precision in the ADNI cohort. NeuroImage 49, 2123–2133.
Lenroot, R.K., Schmitt, J.E., Ordaz, S.J., Wallace, G.L., Neale, M.C., Lerch, J.P., Kendler, K.S., Evans, A.C., Giedd, J.N., 2007. Differences in genetic and environmental influences on the human cerebral cortex associated with development during childhood and adolescence. Hum. Brain Mapp.
Magnaldi, S., Ukmar, M., Vasciaveo, A., Longo, R., Pozzi-Mucelli, R.S., 1993. Contrast between white and grey-matter: MRI appearance with ageing. Eur. J. Radiol. 3, 513–519.
Narr, K.L., Bilder, R.M., Toga, A.W., Woods, R.P., Rex, D.E., Szeszko, P.R., Robinson, D., Sevy, S., Gunduz-Bruce, H., Wang, Y.P., DeLuca, H., Thompson, P.M., 2005. Mapping cortical thickness and gray matter concentration in first episode schizophrenia. Cereb. Cortex 15, 708–719.
Neale, M.C., Cardon, L.R., 1992. Methodology for Genetic Studies of Twins and Families. Kluwer Academic Publishers, Dordrecht, The Netherlands.
Panizzon, M.S., Fennema-Notestine, C., Eyler, L.T., Jernigan, T.L., Prom-Wormley, E., Neale, M., Jacobson, K., Lyons, M.J., Grant, M.D., Franz, C.E., Xian, H., Tsuang, M., Fischl, B., Seidman, L., Dale, A., Kremen, W.S., 2009. Distinct genetic influences on cortical surface area and cortical thickness. Cereb. Cortex.
Peper, J.S., Brouwer, R.M., Boomsma, D.I., Kahn, R.S., Hulshoff Pol, H.E., 2007. Genetic influences on human brain structure: a review of brain imaging studies in twins. Hum. Brain Mapp. 28, 464–473.
Raz, N., Millman, D., Sarpel, G., 1990. Cerebral correlates of cognitive aging: gray–white-matter differentiation in the medial temporal lobes, and fluid versus crystallized abilities. Psychobiology 18, 475–481.
Rimol, L.M., Panizzon, M.S., Fennema-Notestine, C., Fischl, B., Franz, C.E., Lyons, M.J., Makris, N., Neale, M.C., Pacheco, J., Perry, M.E., Schmitt, J.E., Seidman, L., Thermenos, H.W., Tsuang, M.T., Kremen, W.S., Dale, A.M., 2009. Cortical thickness is influenced by regionally specific genetic factors. Biol. Psychiatry 67, 493–499.
Salat, D.H., Buckner, R.L., Snyder, A.Z., Greve, D.N., Desikan, R.S., Busa, E., Morris, J.C., Dale, A.M., Fischl, B., 2004. Thinning of the cerebral cortex in aging. Cereb. Cortex 14, 721–730.
Salat, D.H., Chen, J.J., van der Kouwe, A.J., Greve, D.N., Fischl, B., Rosas, H.D., 2011. Hippocampal degeneration is associated with temporal and limbic gray matter/white matter tissue contrast in Alzheimer's disease. NeuroImage 54, 1795–1802.
Salat, D.H., Lee, S.Y., van der Kouwe, A.J., Greve, D.N., Fischl, B., Rosas, H.D., 2009. Age-associated alterations in cortical gray and white matter signal intensity and gray to white matter contrast. NeuroImage 48, 21–28.
Schmitt, J.E., Eyler, L.T., Giedd, J.N., Kremen, W.S., Kendler, K.S., Neale, M.C., 2007a. Review of twin and family studies on neuroanatomic phenotypes and typical neurodevelopment. Twin Res. Hum. Genet. 10, 683–694.
Schmitt, J.E., Lenroot, R.K., Wallace, G.L., Ordaz, S., Taylor, K.N., Kabani, N., Greenstein, D., Lerch, J.P., Kendler, K.S., Neale, M.C., Giedd, J.N., 2008. Identification of genetically mediated cortical networks: a multivariate study of pediatric twins and siblings. Cereb. Cortex 18, 1737–1747.
Schmitt, J.E., Wallace, G.L., Rosenthal, M.A., Molloy, E.A., Ordaz, S., Lenroot, R., Clasen, L.S., Blumenthal, J.D., Kendler, K.S., Neale, M.C., Giedd, J.N., 2007b. A multivariate analysis of neuroanatomic relationships in a genetically informative pediatric sample. NeuroImage 35, 70–82.
Self, S.G., Liang, K.L., 1987. Asymptotic properties of maximum likelihood estimators and likelihood ratio tests under nonstandard conditions. J. Am. Stat. Assoc. 82, 605–610.
Steiger, J.H., Shapiro, A., Browne, M.W., 1985. On the multivariate asymptotic-distribution of sequential chi-square statistics. Psychometrika 50, 253–264.
Stonnington, C.M., Tan, G., Kloppel, S., Chu, C., Draganski, B., Jack, C.R., Chen, K., Ashburner, J., Frackowiak, R.S., 2008. Interpreting scan data acquired from multiple scanners: a study with Alzheimer's disease. NeuroImage 39, 1180–1185.

Westlye, L.T., Walhovd, K.B., Dale, A.M., Bjornerud, A., Due-Tonnessen, P., Engvig, A., Grydeland, H., Tamnes, C.K., Ostby, Y., Fjell, A.M., 2010. Differentiating maturational and aging-related changes of the cerebral cortex by use of thickness and signal intensity. NeuroImage 52, 172–185.

Westlye, L.T., Walhovd, K.B., Dale, A.M., Espeseth, T., Reinvang, I., Raz, N., Agartz, I., Greve, D.N., Fischl, B., Fjell, A.M., 2009. Increased sensitivity to effects of normal aging and Alzheimer's disease on cortical thickness by adjustment for local variability in gray/white contrast: a multi-sample MRI study. NeuroImage.

Winkler, A.M., Kochunov, P., Blangero, J., Almasy, L., Zilles, K., Fox, P.T., Duggirala, R., Glahn, D.C., 2010. Cortical thickness or grey matter volume? The importance of selecting the phenotype for imaging genetics studies. NeuroImage.

Wonderlick, J.S., Ziegler, D.A., Hosseini-Varnamkhasti, P., Locascio, J.J., Bakkour, A., van der Kouwe, A., Triantafyllou, C., Corkin, S., Dickerson, B.C., 2009. Reliability of MRI-derived cortical and subcortical morphometric measures: effects of pulse sequence, voxel geometry, and parallel imaging. NeuroImage 44, 1324–1333.